

## Spectroscopy along Flerovium Decay Chains: Discovery of $^{280}\text{Ds}$ and an Excited State in $^{282}\text{Cn}$

A. Sămark-Roth<sup>1,\*</sup>, D. M. Cox,<sup>1</sup> D. Rudolph,<sup>1</sup> L. G. Sarmiento,<sup>1</sup> B. G. Carlsson,<sup>1</sup> J. L. Egido,<sup>2</sup> P. Golubev,<sup>1</sup> J. Heery,<sup>3</sup> A. Yakushev,<sup>4</sup> S. Åberg,<sup>1</sup> H. M. Albers,<sup>4</sup> M. Albertsson,<sup>1</sup> M. Block,<sup>4,5,6</sup> H. Brand,<sup>4</sup> T. Calverley,<sup>3</sup> R. Cantemir,<sup>4</sup> R. M. Clark,<sup>7</sup> Ch. E. Düllmann,<sup>4,5,6</sup> J. Eberth,<sup>8</sup> C. Fahlander,<sup>1</sup> U. Forsberg,<sup>1</sup> J. M. Gates,<sup>7</sup> F. Giacoppo,<sup>4,5</sup> M. Götz,<sup>4,5,6</sup> S. Götz,<sup>4,5,6</sup> R.-D. Herzberg,<sup>3</sup> Y. Hrabar,<sup>1</sup> E. Jäger,<sup>4</sup> D. Judson,<sup>3</sup> J. Khuyagbaatar,<sup>4,5</sup> B. Kindler,<sup>4</sup> I. Kojouharov,<sup>4</sup> J. V. Kratz,<sup>6</sup> J. Krier,<sup>4</sup> N. Kurz,<sup>4</sup> L. Lens,<sup>4,6,†</sup> J. Ljungberg,<sup>1</sup> B. Lommel,<sup>4</sup> J. Louko,<sup>9</sup> C.-C. Meyer,<sup>5,6</sup> A. Mistry,<sup>10,4</sup> C. Mokry,<sup>5,6</sup> P. Papadakis,<sup>3,‡</sup> E. Parr,<sup>4</sup> J. L. Pore,<sup>7</sup> I. Ragnarsson,<sup>1</sup> J. Runke,<sup>4,6</sup> M. Schädel,<sup>4</sup> H. Schaffner,<sup>4</sup> B. Schausten,<sup>4</sup> D. A. Shaughnessy,<sup>11</sup> P. Thörle-Pospiech,<sup>5,6</sup> N. Trautmann,<sup>6</sup> and J. Uusitalo<sup>9</sup>

<sup>1</sup>Department of Physics, Lund University, 22100 Lund, Sweden

<sup>2</sup>Departamento de Física Teórica and CIAFF, Universidad Autónoma de Madrid, 28049 Madrid, Spain

<sup>3</sup>Department of Physics, University of Liverpool, Liverpool L69 7ZE, United Kingdom

<sup>4</sup>GSI Helmholtzzentrum für Schwerionenforschung GmbH, 64291 Darmstadt, Germany

<sup>5</sup>Helmholtz Institute Mainz, 55099 Mainz, Germany

<sup>6</sup>Department Chemie–Standort TRIGA, Johannes Gutenberg-Universität Mainz, 55099 Mainz, Germany

<sup>7</sup>Nuclear Science Division, Lawrence Berkeley National Laboratory, Berkeley, California 94720, USA

<sup>8</sup>Institut für Kernphysik, Universität zu Köln, 50937 Köln, Germany

<sup>9</sup>Department of Physics, University of Jyväskylä, 40014 Jyväskylä, Finland

<sup>10</sup>Institut für Kernphysik, Technische Universität Darmstadt, 64289 Darmstadt, Germany

<sup>11</sup>Nuclear and Chemical Sciences Division, Lawrence Livermore National Laboratory, Livermore, California 94550, USA



(Received 16 November 2020; accepted 3 December 2020; published 22 January 2021)

A nuclear spectroscopy experiment was conducted to study  $\alpha$ -decay chains stemming from isotopes of flerovium (element  $Z = 114$ ). An upgraded TASI Spec decay station was placed behind the gas-filled separator TASCAs at the GSI Helmholtzzentrum für Schwerionenforschung in Darmstadt, Germany. The fusion-evaporation reactions  $^{48}\text{Ca} + ^{242}\text{Pu}$  and  $^{48}\text{Ca} + ^{244}\text{Pu}$  provided a total of 32 flerovium-candidate decay chains, of which two and eleven were firmly assigned to  $^{286}\text{Fl}$  and  $^{288}\text{Fl}$ , respectively. A prompt coincidence between a 9.60(1)-MeV  $\alpha$  particle event and a 0.36(1)-MeV conversion electron marked the first observation of an excited state in an even-even isotope of the heaviest man-made elements, namely  $^{282}\text{Cn}$ . Spectroscopy of  $^{288}\text{Fl}$  decay chains fixed  $Q_\alpha = 10.06(1)$  MeV. In one case, a  $Q_\alpha = 9.46(1)$ -MeV decay from  $^{284}\text{Cn}$  into  $^{280}\text{Ds}$  was observed, with  $^{280}\text{Ds}$  fissioning after only 518  $\mu\text{s}$ . The impact of these findings, aggregated with existing data on decay chains of  $^{286,288}\text{Fl}$ , on the size of an anticipated shell gap at proton number  $Z = 114$  is discussed in light of predictions from two beyond-mean-field calculations, which take into account triaxial deformation.

DOI: 10.1103/PhysRevLett.126.032503

Experimental studies of superheavy atomic nuclei at the present limits of proton number  $Z$  and mass number  $A$  are of fundamental significance for chemistry and physics. Following the approval and naming of elements up to  $Z = 118$  (oganesson, Og) [1], the hunt for new elements with proton numbers  $Z \geq 119$  has intensified. In parallel, there are continued efforts to collect increasingly detailed information on chemical and physical properties of these rare

species. Comprehensive overviews of the field, summarizing state-of-art experimental methods and theoretical approaches, can be found in, for instance, Refs. [2,3].

Elements 114 (flerovium, Fl) and 115 (moscovium, Mc) play a special role in the context of the detailed investigations. The main reason is that production cross sections for a number of their isotopes were firmly established to be rather high at  $\sigma_{\text{prod}} \approx 5\text{--}10$  pb [4,5]. In the case of Fl, considerable efforts were undertaken to establish chemical properties [6–9]. In the case of Mc, primarily the decay chain associated with  $^{288}\text{Mc}$  was subject to nuclear spectroscopy studies [10,11]. Supported by Monte Carlo simulations [12], decay schemes based on  $\alpha$ -photon coincidences were proposed along the  $^{288}\text{Mc}$  decay chain [10,13], followed

Published by the American Physical Society under the terms of the Creative Commons Attribution 4.0 International license. Further distribution of this work must maintain attribution to the author(s) and the published article's title, journal citation, and DOI.

by contemporary nuclear theory assessments [14]. More recently, the mass number  $A = 288$  was directly measured for that decay chain [15].

Nuclear spectroscopy results on Fl isotopes are relevant for nuclear theory. Most microscopic-macroscopic models see  $Z = 114$  as magic proton number, typically in combination with neutron number  $N = 184$ , while a majority of modern mean-field approaches prefer  $Z = 120$  [2,16,17]. At spherical deformation, an extended region of low level density and shell corrections is expected for  $114 \leq Z \leq 120$  by most models. However, the heaviest flerovium isotope in experimental reach at present is  $^{290}\text{Fl}$  with  $N = 176$ , i.e., still eight neutrons short of the anticipated doubly magic core  $^{298}\text{Fl}$ . Whether or not the isotopes in experimental reach are near spherical, well deformed, or show aspects of shape coexistence, is one of the key questions that remains to be tackled.

In this Letter, we report on newly observed decay properties along  $^{286}\text{Fl}$  and  $^{288}\text{Fl}$  decay chains stemming from a high-resolution spectroscopy experiment. Results from the same experiment on the odd- $A$  isotope  $^{289}\text{Fl}$  will be published separately [18]. Notes on preparatory efforts and some calibration procedures can be found in Ref. [19], while Ref. [20] provides further details on data analysis and statistical assessments. The Supplemental Material to this Letter [21] summarizes key information on previous and present results on the decay chains of interest.

The Universal Linear Accelerator (UNILAC) at the GSI Helmholtzzentrum für Schwerionenforschung, Darmstadt, Germany, delivered a beam of  $^{48}\text{Ca}^{10+}$  ions with a typical intensity of  $5 \times 10^{12}$  particles per second, time averaged over its pulsed structure, 5 ms beam on and 15 ms beam off. A beam integral of  $6.0(4) \times 10^{18}$  ions was collected in two experimental runs. With an initial energy of  $6.021(2)$  MeV/u, then degraded by Ti foils with thicknesses indicated in Table I, the  $^{48}\text{Ca}$  beam impinged

on a rotating target wheel [22]. The latter comprised four segments of either enriched  $^{242}\text{Pu}$  ( $> 99.5\%$ ) or  $^{244}\text{Pu}$  ( $> 98.5\%$ ). The Pu material was deposited by molecular plating on 2.2- and 2.3- $\mu\text{m}$  thick Ti foils [23]. The Ti foils faced the degraded beam. In the first run, a mixed target wheel with one  $^{242}\text{PuO}_2$  and three  $^{244}\text{PuO}_2$  segments was used. The second run had only  $^{244}\text{PuO}_2$  segments mounted onto the wheel. Table I provides an overview of thicknesses of degrader foils, backing foils, and target layers, as well as derived midtarget beam energies and beam integrals.

Behind the target wheel, the recoil separator TASCA [26] was used to direct reaction products toward an upgraded version [19] of the TASI Spec decay station [27]. TASCA was filled with 0.8 mbar He gas and was set to center ions in the focal plane with a magnetic rigidity of  $B\rho = 2.27$  Tm [8,9,28]. Transmission of Fl fusion-evaporation residues from the target wheel into TASI Spec was estimated to be 30(3)% [29,30].

The core of TASI Spec is a cubelike arrangement of a 0.31-mm thick,  $32 \times 32$ -strip double-sided silicon strip detector (DSSD) and four additional 0.97 mm thick,  $16 \times 16$ -strip DSSDs placed upstream. A second 0.31-mm DSSD was placed behind the central implantation DSSD to veto background radiation from, for instance,  $\beta$  decays of transfer reaction products during beam-off periods [19]. All six DSSD wafers are  $60 \times 60$  mm<sup>2</sup> in area, including a surrounding 1-mm wide guard ring, 80- $\mu\text{s}$  traces of the 256 preamplified signals were recorded by 50-MHz, 14-bit sampling digitizers. Five composite germanium detectors were placed closely behind each of the five sides of the DSSD cube—one seven-crystal Cluster detector [31] downstream, and four novel four-crystal Compex detectors [32] behind each of the upstream DSSDs. Their signals were processed by 100-MHz, 16-bit sampling digitizers, while only flattop energy, baseline, time, and a pileup recognition flag were recorded.

List mode data were generated once a strip of the implantation detector registered a signal above a threshold of  $\approx 150$  keV, or alternatively when one of the four upstream DSSDs registered a signal in excess of  $\approx 5$  MeV. Trigger rates were typically  $\approx 1200$  ( $\approx 150$ ) events per second during beam-on (beam-off) periods. In case the detection of a 9.5–10.3-MeV  $\alpha$  particle in the DSSD cube engaged the same pixel of the implantation detector as a preceding recoil candidate within 20 s and during a beam-off period, an electrostatic chopper near the ion source was activated to bend the beam away from the axis within 20  $\mu\text{s}$ . This allowed for low-background measurements of subsequent decays up to 200 or 300 s for the first or second part of the experiment, respectively. Event trigger type, beam on-off status, in-beam target segment, activated chopper, and various detector and event rates were recorded as well. Details on analysis aspects can be found in Refs. [19,20].

For the even-even isotopes  $^{286,288}\text{Fl}$ , a search for time- and position-correlated recoil- $\alpha(-\alpha)$ -fission sequences was

TABLE I. Summary of Pu target segments, Ti backing and degrader thicknesses, midtarget beam energies and compound-nucleus excitation energies <sup>c</sup>, measured beam integrals, and number of decay chains associated with  $^{286,288}\text{Fl}$ .

Target <sup>a</sup>	$^{242}\text{Pu}$		$^{244}\text{Pu}$	
Pu layer (mg/cm <sup>2</sup> )	0.71(1)		0.80(1)	
Ti backing ( $\mu\text{m}$ )	$1 \times 2.3(1)$		$3 \times 2.3(1); 1 \times 2.2(1)$	
Experiment part	Only Run 1		Run 1 and Run 2	
Ti degrader ( $\mu\text{m}$ )	5.0(1)	5.5(1)	5.1(1)	5.6(1)
$\langle E_{\text{beam}} \rangle$ <sup>b</sup> (MeV)	241.2	238.0	240.6	237.4
$E_{\text{CN,min}}^*$ <sup>c</sup> (MeV)	34.7	32.1	35.7	33.1
$E_{\text{CN,max}}^*$ <sup>c</sup> (MeV)	40.8	38.2	42.5	39.9
Beam integral ( $10^{18}$ )	0.19(1)	0.26(2)	2.23(13)	3.29(19)
No. $^{286,288}\text{Fl}$ chains	2	...	6	$5 + 1$ <sup>d</sup>

<sup>a</sup>For more information, see Ref. [20].

<sup>b</sup>Energy losses were simulated with SRIM [24] and have  $\approx 2$  MeV systematic uncertainty.

<sup>c</sup>Masses of compound nuclei  $^{290,292}\text{Fl}$  taken from [25].

<sup>d</sup>The ambiguous  $^{286}\text{Fl}$  or  $^{288}\text{Fl}$  chain was included here [21].

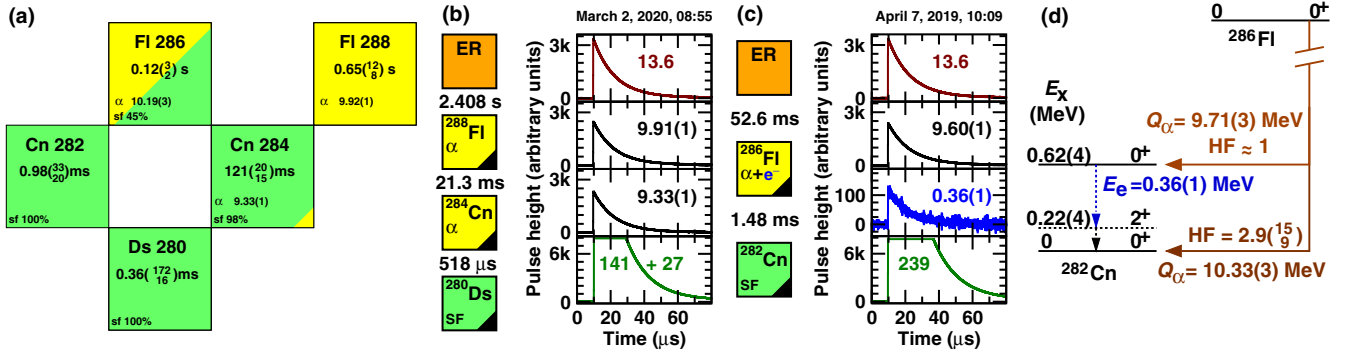


FIG. 1. (a) Summary of the decay chains of  $^{286,288}\text{Fl}$  (cf. Supplemental Material [21] and Table II). (b),(c) Digitized preamplifier pulses of events associated with decay chains 08 and 02. Numbers in the panels are calibrated energies in mega-electron volts. Correlation times are given between recoil implantation (orange squares),  $\alpha$  decays (yellow squares), and fission (green squares). The 0.36(1)-MeV event in an upstream DSSD (blue) is in prompt coincidence with the 9.60(1)-MeV event in the implantation DSSD. Black triangles in the lower right corner of a square indicate detection during beam-off periods. (d) Suggested decay sequence of chain 02 through excited states of  $^{282}\text{Cn}$ . Tentative levels and transitions are dashed.

conducted using the following criteria: (i)  $11.0 < E_{\text{rec}} < 20.0$  MeV, beam on; (ii)  $9.4 < E_{\alpha 1} < 10.5$  MeV,  $\Delta t_{\text{rec}-\alpha 1} \leq 7$  s, beam on or off; (iii)  $E_{\text{SF}} < 300$  MeV beam off or  $150 < E_{\text{SF}} < 250$  MeV beam on,  $\Delta t_{\alpha 1-\text{SF}} \leq 1$  s. Here,  $\alpha$ -particle energies concern both full-energy  $\alpha$  events in the implantation detector as well as those reconstructed between implantation and any upstream DSSD. Throughout the whole experiment, as few as 44 beam-off fission events were registered. Hence, these 44 events as well as candidate chains arising from the search were investigated in more detail, in particular for additional  $\alpha$ -escape events between recoil and concluding fission, as well as photons or (conversion) electrons in prompt coincidence with any decay event. Taking into account the pulsed beam structure of UNILAC, the option for extended beam-off periods (see above), and the possibility of missing events due to data-acquisition dead time, a

decision tree yielded a probability of  $\approx 93\%$  to identify  $^{286,288}\text{Fl}$  decay chains as shown in Fig. 1(a) [20].

The experimental results concerning the fourteen observed  $^{286,288}\text{Fl}$  decay chains are detailed in Table I in the Supplemental Material [21]. Out of a total of 32 candidate flerovium decay chains (30 of which with concluding beam-off fission), two were firmly assigned to  $^{286}\text{Fl}$  (chains 01 and 02), eleven to  $^{288}\text{Fl}$  (chains 04–14), and one to either  $^{286}\text{Fl}$  or  $^{288}\text{Fl}$  (chain 03, ambiguous  $\alpha$ -decay energy). Prompt ( $\Delta t < 300$  ns)  $\alpha$ -photon coincidences were not observed along these fourteen decay chains. The remaining eighteen decay chains are candidates to start from the odd- $A$  isotope  $^{289}\text{Fl}$  [18].

Figure 1(a) and Table II summarize the current status of all previously reported direct and indirect observations of  $^{286}\text{Fl}$  [33–39] and  $^{288}\text{Fl}$  [4,8,9,28,33,37,40–42]. For details we refer to Figs. 1 and 2 and Table II of the Supplemental

TABLE II. Summary of aggregated experimental results concerning the decays of  $^{292}\text{Lv}$ ,  $^{288}\text{Fl}$ ,  $^{286}\text{Fl}$ , and  $^{284}\text{Cn}$ .

$E_\alpha$ (MeV)	$Q_\alpha$ (MeV)	$T_{1/2}$ (s)	$b_\alpha$ <sup>a</sup>	$T_{1/2}(\alpha)$ <sup>b</sup> (s)	HF <sup>b</sup> [44]	$T_{1/2}(\text{SF})$ <sup>b</sup> (ms)
$^{292}\text{Lv}$ [40–42]:						
10.64(4)	10.79(4)	0.013( <sub>3</sub> <sup>6</sup> )	1	0.013( <sub>3</sub> <sup>6</sup> )	0.7( <sub>3</sub> <sup>6</sup> )	Not applicable
$^{288}\text{Fl}$ [21]:						
9.92(1)	10.06(1)	0.65( <sub>8</sub> <sup>12</sup> )	1	0.65( <sub>8</sub> <sup>12</sup> )	1.6( <sub>3</sub> <sup>4</sup> )	Not applicable
$^{284}\text{Cn}$ [21]:						
9.33(1)	9.46(1)	0.121( <sub>15</sub> <sup>20</sup> )	1/51	6.1( <sub>8</sub> <sup>10</sup> )	1.1( <sub>2</sub> <sup>3</sup> )	0.123( <sub>15</sub> <sup>20</sup> )
$^{286}\text{Fl}$ [21]:						
10.19(3)	10.33(3)	0.121( <sub>21</sub> <sup>31</sup> )	15/29	0.23( <sub>4</sub> <sup>6</sup> )	2.9( <sub>9</sub> <sup>15</sup> )	0.27( <sub>5</sub> <sup>7</sup> )
9.57(3) <sup>c</sup>	9.71(3)		1/29	3.5( <sub>6</sub> <sup>9</sup> )	$\approx 1$	

<sup>a</sup>Because of incomplete knowledge from previous studies, the branching ratio can only be estimated from cases of hitherto reported types of decay chains.

<sup>b</sup>The uncertainties cannot account for uncertainties in branching ratios. See preceding note.

<sup>c</sup>The observed 9.60(1) MeV are attributed to the summing of a 9.57(3) MeV  $\alpha$ -decay energy and 0.03(2) MeV related to atomic electron relaxation processes because of the two internal conversion decays as suggested in Fig. 1(d).

Material [21], which provide the spectral and statistical analyses of five data ensembles of the decays of  $^{286,288}\text{Fl}$  and  $^{282,284}\text{Cn}$ : (i) previous direct production; (ii) previous indirect production; (iii) combination of ensembles (i) and (ii); (iv) present data; and (v) combination of ensembles (iii) and (iv). Based on the results of the extended Schmidt test [43] shown in Table II in the Supplemental Material, all five ensembles and all assigned chains and decay steps within the respective ensemble were found to be consistent.

One note is, however, in order: irrespective of either direct or indirect production of  $^{288}\text{Fl}$ , there seemed to be hints for two closely lying decay paths ( $\Delta E \approx 0.1$  MeV) of similar strength [cf. Figs. 2(a), 2(d), 2(g), Ref. [21]] in all earlier data sets [45]. The present data set resolves that puzzling observation. Superior spectroscopic quality in combination with the comparatively large amount of data points yielded a single  $\alpha$ -decay line at 9.92(1) MeV with a full-width at half maximum of 35 keV [cf. Fig. 2(j) Ref. [21]], thus fixing the decay characteristics of  $^{288}\text{Fl}$  [cf. Fig. 1(a) and Table II].

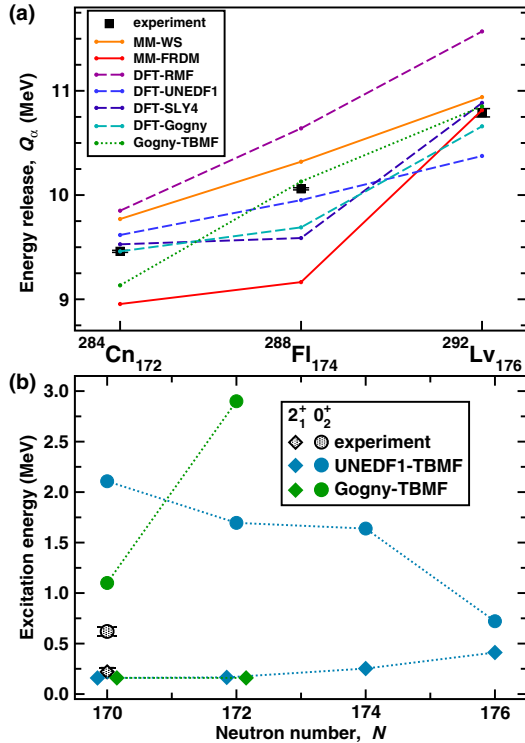


FIG. 2. (a) Comparison of observed and predicted  $Q_\alpha$  values of the  $\alpha$ -decay sequence  $^{292}\text{Lv}$ ,  $^{288}\text{Fl}$ , and  $^{284}\text{Cn}$ . The theoretical numbers stem from macroscopic-microscopic (MM) models [48,49], axially symmetric (SLY4 and UNEDF1 [50], Gogny [51]) and triaxial (RMF [52]) density functional theory (DFT), and a triaxial beyond-mean-field (TBMF) description [54]. (b) Proposed excited states in  $^{282}\text{Cn}$  compared with predictions of two TBMF calculations [54,55] for  $2_1^+$  (diamonds) and  $0_2^+$  states (circles) in  $N = 170-176$ ,  $^{282-288}\text{Cn}$ . The predicted  $E(2^+)$  values for  $^{282,284}\text{Cn}$  are nearly identical for both descriptions and were therefore placed side by side.

Two decay chains, number 08 assigned to  $^{288}\text{Fl}$  and number 02 assigned to  $^{286}\text{Fl}$ , are of particular interest. Their observed implantation and decay series are illustrated in Figs. 1(b) and 1(c).

Chain 08 is built upon a recoil implantation of 13.6 MeV, followed by a presumed full-energy  $\alpha$ -decay event,  $E_{\alpha 1} = 9.91(1)$  MeV, after 2.408 s during a beam-off period. This event triggered the beam shut-off routine. After 21.3 ms, another presumed full-energy  $\alpha$ -decay event,  $E_{\alpha 2} = 9.33(1)$  MeV, was detected, with a fission event following only 518  $\mu\text{s}$  later. For this event, one fission fragment left the implantation detector (141 MeV signal) and reached an upstream detector (27 MeV signal). With the first  $\alpha$ -decay energy and both first correlation times being consistent with  $^{288}\text{Fl}$  and  $^{284}\text{Cn}$  averages, we conclude to have for the first time observed an  $\alpha$ -decay branch [ $Q_\alpha = 9.46(1)$  MeV,  $b_\alpha = 1/51 \approx 2\%$ ] from  $^{284}\text{Cn}$  into  $^{280}\text{Ds}$ , which is found to fission with  $T_{1/2} = 0.36_{(16)}^{(172)}$  ms [46]. The random probability of observing this recoil- $\alpha$ -fission decay sequence in our experiment was as low as  $3 \times 10^{-12}$  [20]. Together with existing information on  $^{292}\text{Lv}$  [40-42], this decay chain firmly establishes the first high-resolution  $Q_\alpha$  sequence across  $Z = 114$  (cf. Table II) [47].

Figure 2(a) compares the newly established  $^{292}\text{Lv}$ - $^{288}\text{Fl}$ - $^{284}\text{Cn}$ - $^{280}\text{Ds}$   $Q_\alpha$  series with a selection of predictions, namely from macroscopic-microscopic (MM) approaches [48,49], various nonrelativistic density-functional theories (DFT) with different interactions [50,51], a relativistic one [52], and a first fully triaxial beyond-mean-field (TBMF) calculation [53,54].

Notably, the measured  $Q_\alpha$  values pass smoothly through  $Z = 114$ , which is at variance with some MM descriptions, for example [48], with a pronounced  $Z = 114$  shell gap and thus near-spherical shapes around  $N = 174$ . Similarly, several axially symmetric DFT with the Skyrme (SLY4) and Gogny (D1S) interactions predict a “kink” of  $Q_\alpha$  at  $^{288}\text{Fl}$  as well, although they do not predict a  $Z = 114$  gap. Since triaxial shapes are important in these nuclei [54,56], we extended the axially symmetric Gogny calculations of Ref. [51] to include triaxial shapes. The results, not displayed here, show the persistence of the kink indicating that triaxiality is at least not the only reason for the discrepancy with experimental data. In turn, MM predictions based on a Woods-Saxon potential [49], the unified energy-density Skyrme functional (UNEDF1) [50], and the triaxial relativistic mean-field (RMF) model [52], respectively, are schematically consistent with the smooth experimental trend across  $Z = 114$ . However, slopes and absolute values remain different, as can be seen in Fig. 2(a).

The TBMF calculations [53] were performed with the Gogny force and provide a good description of the experimental data: the  $Q_\alpha$  values for  $^{288}\text{Fl}$  and  $^{292}\text{Lv}$  agree with the experiment, while the one for  $^{284}\text{Cn}$  is somewhat too small. These calculations were performed using a configuration space of thirteen major harmonic oscillator

shells. We note, however, that although this size is sufficient to reach relative convergence, it is not evident that absolute convergence of the total binding energies, in particular for the more deformed lighter nuclei, was reached.

All models showing an almost linear trend in  $Q_\alpha$  values also predict weakly deformed, near-prolate shapes with  $\beta \approx 0.15$ . The absence of a kink indicates that no pronounced shell effect from crossing  $Z = 114$  is observed (at  $N = 174$ ). This may provide an upper limit of the size of the proposed  $Z = 114$  gap at this neutron number.

Hindrance factors (HF) along this decay sequence are listed in Table II, calculated with respect to a modified Geiger-Nuttall relation [44]. The HF values are close to unity, with  $^{288}\text{Fl}$  mildly deviating. This indicates in general similar wave functions of the involved mother and daughter  $0_1^+$  ground states.

The detection of chain 02, shown in Fig. 1(c), started with a recoil implantation of 13.6 MeV, followed by a presumed  $\alpha$ -decay event of 9.60(1) MeV after 52.6 ms during a beam-off period. This event triggered the beam shut-off routine. After 1.48 ms, a fission event concluded the chain, with 239 MeV measured in the implantation DSSD. The random probability of observing such a sequence in our experiment was  $8 \times 10^{-7}$  [20]. While the recoil- $\alpha$  and  $\alpha$ -SF correlation times are perfectly compatible with the half lives known for the decay chain of  $^{286}\text{Fl}$ , the 9.60(1) MeV is  $\approx 0.6$  MeV below the present best value  $E_\alpha(^{286}\text{Fl}) = 10.19(3)$  MeV [21].

The unique point of this decay chain is the detection of a 0.36(1) MeV signal in one pixel of the upstream detectors in prompt coincidence,  $\Delta t < 50$  ns, with the 9.60(1)-MeV event in the implantation detector. Recoil implantation depth and pixel-to-pixel direction exclude the possibility of a to-be-reconstructed  $\alpha$ -particle event [20]. Thus, the only explanation for the observed event is an  $\alpha$ -(conversion)electron coincidence. Second, a study of all possible  $\alpha$ - $e^-$  events provided a very conservative upper limit of  $< 1\%$  probability for the observed 9.60(1)-0.36(1)-MeV coincidence being random [20]. Finally,  $[9.60(1) + 0.36(1)]$  MeV +  $B_{e,K,L}(\text{Cn}) \approx E_\alpha(^{286}\text{Fl})$ . In conjunction with the very short correlation times, an explanation for this observation is an  $E_\alpha \approx 9.6$  MeV branch with  $b_\alpha = 1/29 \approx 3\%$ , which connects the  $0^+$  ground state of  $^{286}\text{Fl}$  with an excited state of  $^{282}\text{Cn}$ , located at  $\approx 0.6$  MeV excitation energy (cf. Table II for  $Q_\alpha$ ). In this scenario, the 0.36(1) MeV  $e^-$  is arising from a converted electromagnetic transition.

The hindrance factor [44] of a  $0_1^+ \rightarrow 0_2^+$  branch turns out to be close to unity, while the observation of a finite  $\Delta\mathcal{L}_\alpha \neq 0$   $\alpha$ -particle branch with  $\approx 0.6$  MeV less energy is considerably less likely. Therefore, spin-parity  $I^\pi = 0^+$  is suggested for the excited state at  $\approx 0.6$  MeV. The excitation energy of the first  $2^+$  state in  $^{282}\text{Cn}$  is expected at lower energy, in fact  $E(2_1^+) \ll 0.6$  MeV [see, e.g., Fig. 2(b) and

Refs. [48–52]]. The presence of a  $2_1^+$  state below the excited  $0_2^+$  state implies that the decay of the latter proceeds with high probability via an  $E2$  cascade passing through the  $2^+$  state. This is illustrated in Fig. 1(d), which presents this tentative decay scenario [20]. Conversion coefficients are calculated at  $\alpha_{\text{tot}} \approx 2.6$  and 0.33 for 220- and 400-keV [57], respectively [57]. Even in case both conversion electrons, most likely of  $L2$  character, are emitted backward, atomic relaxation processes are likely to contribute some energy to the measured 9.60(1) MeV event in the implantation DSSD. The summed electron energy contribution is estimated to 0.03(2) MeV [58,59]. This leaves  $E_\alpha = 9.57(3)$  MeV [corresponding to  $Q_\alpha = 9.71(3)$  MeV] and yields  $E(0_2^+) = 0.62(4)$  MeV and  $E(2_1^+) = 0.22(4)$  MeV for a consistent description of this event.

Figure 2(b) shows the observed and proposed excited states in  $^{282}\text{Cn}$  at 0.62(4) and 0.22(4) MeV in comparison with the sequences of excited  $2_1^+$  and  $0_2^+$  states predicted by two contemporary triaxial beyond-mean-field approaches: Gogny TBMF is based on the effective finite-range density-dependent Gogny force and UNEDF1 TBMF relies on mapping the Skyrme functional to a separable Hamiltonian. Both sets of calculations restore the particle number and angular momentum symmetries and incorporate the mixing of triaxial shapes by means of the generator coordinate method (GCM). For details we refer to Refs. [53–55]. In fact, a fully triaxial approach is called for, since restricted axially symmetric calculations for superheavy nuclei predict oblate and prolate shapes at similar values of  $\beta$ . The question and quest for shape coexistence comes to mind, eventually by means of low-lying  $0^+$  states as observed, for instance, in  $^{186}\text{Pb}$  [60] or  $^{188,192}\text{Po}$  [61].

Both calculations predict smoothly increasing  $2_1^+$  energies, i.e., decreasing quadrupole deformation with increasing neutron number. However, they differ regarding the location of the excited  $0_2^+$  states. While calculated  $0_2^+$  energies are continuously decreasing in the UNEDF1 TBMF approach, the Gogny TBMF calculations predict rather sudden changes of the  $0_2^+$  energy from isotope to isotope, caused by the occurrence of several axially symmetric and triaxial configurations at low energy in these nuclei, similar to what is discussed for the chain of flerovium isotopes in Ref. [54]. Interestingly, just for  $^{282}\text{Cn}$ , a rather low-lying  $0_2^+$  state close to the experimental value is predicted [cf. Fig. 2(b)].

To conclude, an experiment was conducted behind the TASCA separator at GSI Darmstadt, aiming at high-resolution decay spectroscopy of  $Z = 114$  flerovium isotopes. For even-even  $^{288}\text{Fl}$ , a precise  $Q_\alpha$  value was derived. For the first time, an  $\alpha$ -decay branch was observed for  $^{284}\text{Cn}$ . This led to the discovery of  $^{280}\text{Ds}$  and the first determination of a  $Q_\alpha$  series across Fl. This  $Q_\alpha$  series, now completed with a firm data point at  $^{284}\text{Cn}$ , was found to provide a stringent test of model predictions and, in turn, on

the strength of an anticipated (magic) shell gap at proton number  $Z = 114$ . An excited state was observed in the even-even isotope  $^{282}\text{Cn}$ , illustrating the experimental reach of detailed spectroscopy of the heaviest elements. The existence of the state provides yet another anchor point for nuclear theory, because it seems to require an understanding of both shape coexistence and shape transitions for the heaviest elements.

The results presented here are based on the experiment U310, which was performed at the beam line X8/TASCA at the GSI Helmholtzzentrum für Schwerionenforschung, Darmstadt (Germany) in the frame of FAIR Phase-0. The authors would like to thank the ion-source and accelerator staff at GSI for their supreme efforts. This work has received funding from the European Unions Horizon 2020 research and innovation programme under Grant Agreement No. 654002 (ENSAR2). The  $^{244}\text{Pu}$  target material was provided by the U.S. DOE through ORNL. The Lund group is indebted to a decisive grant from the Knut and Alice Wallenberg Foundation (KAW 2015.0021), and we highly appreciate the possibility to work with the workshops at IKP Köln. This work was also supported in part by the Swedish Research Council (Vetenskapsrådet, VR 2016-3969), the Royal Physiographic Society in Lund, the Spanish Ministerio de Ciencia e Innovación under Contract No. FPA2017-84756-C4-2-P, the U.S. DOE under Contract No. DE-AC02-05CH11231 (LBNL), and the UK STFC. DR and JLE appreciate stimulating discussions with A. Jungclaus, CSIC Madrid, and F. P. Heßberger, GSI Darmstadt.

\*Anton.Samark-Roth@nuclear.lu.se

†Present address: Institut für Physikalische Chemie und Radiochemie, Hochschule Mannheim, 68163 Mannheim, Germany.

‡Present address: STFC Daresbury Laboratory, Daresbury, Warrington WA4 4AD, United Kingdom.

- [1] L. Öhrström and J. Reedijk, *Pure Appl. Chem.* **88**, 1225 (2016).
- [2] Special Issue on Superheavy Elements, edited by Ch. E. Düllmann, R.-D. Herzberg, W. Nazarewicz, and Y. Oganessian, *Nucl. Phys.* **A944**, 1 (2015), <https://www.sciencedirect.com/journal/nuclear-physics-a/vol/944>.
- [3] D. Rudolph, EPJ Web Conf. **131** (2016), <https://www.epj-conferences.org/articles/epjconf/abs/2016/26/contents/contents.html>.
- [4] Ch. E. Düllmann, M. Schädel, A. Yakushev, A. Türler, K. Eberhardt, J. V. Kratz *et al.*, *Phys. Rev. Lett.* **104**, 252701 (2010).
- [5] U. Forsberg, D. Rudolph, L.-L. Andersson, A. Di Nitto, Ch. E. Düllmann, C. Fahlander *et al.*, *Nucl. Phys.* **A953**, 117 (2016).
- [6] A. Türler, R. Eichler, and A. Yakushev, *Nucl. Phys.* **A944**, 640 (2015).
- [7] A. Yakushev and R. Eichler, *EPJ Web Conf.* **131**, 07003 (2016).
- [8] A. Yakushev, J. M. Gates, A. Türler, M. Schädel, Ch. E. Düllmann, D. Ackermann *et al.*, *Inorg. Chem.* **53**, 1624 (2014).
- [9] A. Yakushev, L. Lens, Ch. E. Düllmann, H. M. Albers, M. Asai, M. Block *et al.*, *Nat. Chem.* (to be published).
- [10] D. Rudolph, U. Forsberg, P. Golubev, L. G. Sarmiento, A. Yakushev, L.-L. Andersson *et al.*, *Phys. Rev. Lett.* **111**, 112502 (2013).
- [11] J. M. Gates, K. E. Gregorich, O. R. Gothe, E. C. Uribe, G. K. Pang, D. L. Bleuel *et al.*, *Phys. Rev. C* **92**, 021301(R) (2015).
- [12] L. G. Sarmiento, *EPJ Web Conf.* **131**, 05004 (2016).
- [13] D. Rudolph, L. G. Sarmiento, and U. Forsberg, *AIP Conf. Proc.* **1681**, 030015 (2015).
- [14] Yue Shi, D. E. Ward, B. G. Carlsson, J. Dobaczewski, W. Nazarewicz, I. Ragnarsson, and D. Rudolph, *Phys. Rev. C* **90**, 014308 (2014).
- [15] J. M. Gates, G. K. Pang, J. L. Pore, K. E. Gregorich, J. T. KWarsick, G. Savard *et al.*, *Phys. Rev. Lett.* **121**, 222501 (2018).
- [16] J. Dobaczewski, A. V. Afanasjev, M. Bender, L. M. Robledo, and Yue Shi, *Nucl. Phys.* **A944**, 388 (2015).
- [17] P.-H. Heenen, J. Skalski, A. Staszczak, and D. Vretenar, *Nucl. Phys.* **A944**, 415 (2015).
- [18] D. M. Cox *et al.*, *Phys. Rev. Lett.* (to be published).
- [19] D. M. Cox, A. Sâmark-Roth, D. Rudolph, L. G. Sarmiento, C. Fahlander, U. Forsberg *et al.*, *J. Phys. Conf. Ser.* **1643**, 012125 (2020).
- [20] A. Sâmark-Roth *et al.*, *Phys. Rev. C* (to be published).
- [21] See Supplemental Material at <http://link.aps.org/supplemental/10.1103/PhysRevLett.126.032503> for detailed results and statistical assessments concerning decay chains starting with isotopes  $^{286,288}\text{Fl}$ .
- [22] E. Jäger, H. Brand, Ch. E. Düllmann, J. Khuyagbaatar, J. Krier, M. Schädel, T. Torres, and A. Yakushev, *J. Radioanal. Nucl. Chem.* **299**, 1073 (2014).
- [23] J. Runke, Ch. E. Düllmann, K. Eberhardt, P. A. Ellison, K. E. Gregorich, S. Hoffmann *et al.*, *J. Radioanal. Rad. Nucl. Chem.* **299**, 1081 (2014).
- [24] J. F. Ziegler, *Nucl. Instrum. Methods Phys. Res., Sect. B* **219–220**, 1027 (2004).
- [25] W. D. Myers and W. J. Swiatecki, *Nucl. Phys.* **A601**, 141 (1996).
- [26] A. Semchenkov, W. Bröchle, E. Jäger, E. Schimpf, M. Schädel, C. Mühle *et al.*, *Nucl. Instrum. Methods Phys. Res., Sect. B* **266**, 4153 (2008).
- [27] L.-L. Andersson, D. Rudolph, P. Golubev, R.-D. Herzberg, R. Hoischen, E. Merchán *et al.*, *Nucl. Instrum. Methods Phys. Res., Sect. A* **622**, 164 (2010).
- [28] J. M. Gates, Ch. E. Düllmann, M. Schädel, A. Yakushev, A. Türler, K. Eberhardt *et al.*, *Phys. Rev. C* **83**, 054618 (2011).
- [29] U. Forsberg, P. Golubev, L. G. Sarmiento, J. Jeppsson, D. Rudolph, L.-L. Andersson *et al.*, *Acta Phys. Pol.* **43**, 305 (2012).
- [30] K. E. Gregorich, *Nucl. Instrum. Methods Phys. Res., Sect. A* **711**, 47 (2013).
- [31] J. Eberth, H. G. Thomas, P. v. Brentano, R. M. Lieder, H. M. Jäger, H. Kämmerling, M. Berst, D. Gutknecht,

- and R. Henck, *Nucl. Instrum. Methods Phys. Res., Sect. A* **369**, 135 (1996).
- [32] A. Sămark-Roth, D. M. Cox, J. Eberth, P. Golubev, D. Rudolph, L. G. Sarmiento, G. Tocabens, M. Ginsz, B. Pirard, and P. Quirin, *Eur. Phys. J. A* **56**, 141 (2020).
- [33] Yu. Ts. Oganessian, V. K. Utyonkov, Yu. V. Lobanov, F. Sh. Abdullin, A. N. Polyakov, I. V. Shirokovsky *et al.*, *Phys. Rev. C* **70**, 064609 (2004).
- [34] S. Hofmann, D. Ackermann, S. Antalic, H. G. Burkhard, V. F. Comas, R. Dressler *et al.*, *Eur. Phys. J. A* **32**, 251 (2007).
- [35] L. Stavsetra, K. E. Gregorich, J. Dvorak, P. A. Ellison, I. Dragojević, M. A. Garcia, and H. Nitsche, *Phys. Rev. Lett.* **103**, 132502 (2009).
- [36] P. A. Ellison, K. E. Gregorich, J. S. Berryman, D. L. Bleuel, R. M. Clark, I. Dragojević *et al.*, *Phys. Rev. Lett.* **105**, 182701 (2010).
- [37] Yu. Ts. Oganessian, V. K. Utyonkov, Yu. V. Lobanov, F. Sh. Abdullin, A. N. Polyakov, I. V. Shirokovsky *et al.*, *Phys. Rev. C* **69**, 054607 (2004).
- [38] Yu. Ts. Oganessian, V. K. Utyonkov, Yu. V. Lobanov, F. Sh. Abdullin, A. N. Polyakov, R. N. Sagaidak *et al.*, *Phys. Rev. C* **74**, 044602 (2006).
- [39] Yu. Ts. Oganessian, F. Sh. Abdullin, C. Alexander, J. Binder, R. A. Boll, S. N. Dmitriev *et al.*, *Phys. Rev. Lett.* **109**, 162501 (2012).
- [40] Yu. Ts. Oganessian, V. K. Utyonkov, Yu. V. Lobanov, F. Sh. Abdullin, A. N. Polyakov, I. V. Shirokovsky *et al.*, in *JINR, E7-2004-160* (2004), p. 128, [http://www.jinr.ru/publish/Preprints/2004/160\(E7-2004-160\).pdf](http://www.jinr.ru/publish/Preprints/2004/160(E7-2004-160).pdf).
- [41] S. Hofmann, S. Heinz, R. Mann, J. Maurer, J. Khuyagbaatar, D. Ackermann *et al.*, *Eur. Phys. J. A* **48**, 62 (2012).
- [42] D. Kaji, K. Morita, K. Morimoto, H. Haba, M. Asai, K. Fujita *et al.*, *J. Phys. Soc. Jpn.* **86**, 034201 (2017).
- [43] K.-H. Schmidt, *Eur. Phys. J. A* **8**, 141 (2000).
- [44] C. Qi, F. R. Xu, R. J. Liotta, R. Wyss, M. Y. Zhang, C. Asawatangtrakuldee, and D. Hu, *Phys. Rev. C* **80**, 044326 (2009).
- [45] F. P. Heßberger, *EPJ Web Conf.* **131**, 02005 (2016).
- [46] K.-H. Schmidt, C.-C. Sahm, K. Pielenz, and H.-G. Clerc, *Z. Phys. A* **316**, 19 (1984).
- [47] The suggested version B of chain 3 in Ref. [42] has serious problems with both the derived  $\alpha$  energy, correlation time, and in particular the position of the 0.83-MeV escape event tentatively assigned to  $^{288}\text{Fl}$ .
- [48] P. Möller, A. J. Sierk, T. Ichikawa, and H. Sagawa, *At. Data. Nucl. Data Sheets* **109–110**, 1 (2016).
- [49] P. Jachimowicz, M. Kowal, and J. Skalski, *Phys. Rev. C* **89**, 024304 (2014).
- [50] E. Olsen and W. Nazarewicz, *Phys. Rev. C* **99**, 014317 (2019).
- [51] M. Warda and J. L. Egido, *Phys. Rev. C* **86**, 014322 (2012).
- [52] V. Prassa, T. Nikšić, G. A. Lalazissis, and D. Vretenar, *Phys. Rev. C* **86**, 024317 (2012).
- [53] T. R. Rodríguez and J. L. Egido, *Phys. Rev. C* **81**, 064323 (2010).
- [54] J. L. Egido and A. Jungclaus, *Phys. Rev. Lett.* **125**, 192504 (2020).
- [55] B. G. Carlsson and J. Ljungberg, *Phys. Rev. Lett.* (to be published).
- [56] S. Ćwiok, P. H. Heenen, and W. Nazarewicz, *Nature (London)* **433**, 705 (2005).
- [57] T. Kibédi, M. B. Trzhaskovskaya, M. Gupta, and A. E. Stuchberry, *At. Data. Nucl. Data Sheets* **98**, 313 (2012).
- [58] F. P. Heßberger, S. Hoffmann, G. Münzenberg, K.-H. Schmidt, P. Armbruster, and R. Hingmann, *Nucl. Instrum. Methods Phys. Res., Sect. A* **274**, 522 (1989).
- [59] Ch. Theissen, A. Lopez-Martens, and Ch. Bonnelle, *Nucl. Instrum. Methods Phys. Res., Sect. A* **589**, 230 (2008).
- [60] A. N. Andreyev, M. Huyse, P. Van Duppen, L. Weissman, D. Ackermann, J. Gerl *et al.*, *Nature (London)* **405**, 430 (2000).
- [61] K. Van de Vel, A. N. Andreyev, D. Ackermann, H. J. Boardman, P. Cagarda, J. Gerl *et al.*, *Phys. Rev. C* **68**, 054311 (2003).